

Statistical isotropy of CMB anisotropy from WMAP

Tarun Souradeep¹ and Amir Hajian²

*Inter-University Centre for Astronomy and Astrophysics,
Post Bag 4, Ganeshkhind, Pune 411007, India*

Abstract

The statistical expectation values of the temperature fluctuations of cosmic microwave background (CMB) are assumed to be preserved under rotations of the sky. We investigate the statistical isotropy of the CMB anisotropy maps recently measured by the Wilkinson Microwave Anisotropy Probe (WMAP) using bipolar spherical harmonic power spectrum proposed in Hajian & Souradeep 2003. The Bipolar Power Spectrum (BiPS) is estimated for the full sky CMB anisotropy maps of the first year WMAP data. The method allows us to isolate regions in multipole space and study each region independently. This search shows no evidence for violation of statistical isotropy in the first-year WMAP data on angular scales larger than that corresponding to $l \approx 60$.

1 Introduction

In standard cosmology, CMB anisotropy signal is expected to be statistically isotropic, i.e., statistical expectation values of the temperature fluctuations $\Delta T(\hat{q})$ are preserved under rotations of the sky. In particular, the angular correlation function $C(\hat{q}, \hat{q}') \equiv \langle \Delta T(\hat{q}) \Delta T(\hat{q}') \rangle$ is rotationally invariant for Gaussian fields. In spherical harmonic space, where $\Delta T(\hat{q}) = \sum_{lm} a_{lm} Y_{lm}(\hat{q})$ the condition of *statistical isotropy* (SI) translates to a diagonal $\langle a_{lm} a_{l'm'}^* \rangle = C_l \delta_{ll'} \delta_{mm'}$ where C_l , the widely used angular power spectrum of CMB anisotropy. SI CMB sky is essential for C_l to be a complete description of (Gaussian) CMB anisotropy and hence an adequate measure for comparing with models. Hence, it is crucial to be able to determine from the observed CMB sky whether it is a realization of a statistically isotropic process, or not. The detection of statistical isotropy (SI) violations in the CMB signal can have exciting and far-reaching implication for cosmology. For example, a generic consequence of cosmic topology is the breaking of statistical isotropy in characteristic patterns determined by the photon geodesic structure of the manifold as probed by the CMB photons traveling to us from the surface of last scattering over a distance comparable to the cosmic horizon, R_H . On the other hand, SI violation could also arise from foreground contamination, non-cosmological signals and be artifacts of observational technique.

The first-year *Wilkinson Microwave Anisotropy Probe* (WMAP) observations are consistent with predictions of the concordance Λ CDM model with scale-invariant and adiabatic fluctuations which have been generated during the inflationary epoch [Hinshaw et al. 2003, Kogut et al. 2003, Spergel et al. 2003, Page et al. 2003, Peiris et al., 2003]. After the first year of WMAP data, the SI of the CMB anisotropy (i.e. rotational invariance of n-point correlations) has attracted considerable attention. Tantalizing evidence of SI breakdown (albeit, in very different guises) has mounted in the WMAP first year sky maps, using a variety of different statistics. It was pointed out that the suppression of power in the quadrupole and octopole are aligned [Tegmark et al. 2004]. Further “multipole-vector” directions associated with these multipoles (and some other low multipoles as well) appear to be anomalously correlated [Copi et al. 2004, Schwarz et al. 2004]. There are indications of asymmetry in the power spectrum at low multipoles in opposite hemispheres [Eriksen et al. 2004a, Hansen et al. 2004, Naselsky et al. 2004]. Possibly related, are the results of tests of Gaussianity that show asymmetry in the amplitude of the measured genus amplitude (at about 2 to 3σ significance) between the north and south galactic hemispheres [Park 2004, Eriksen et al. 2004b, Eriksen et al. 2004c]. Analysis of the distribution of extrema in WMAP sky maps has indicated non-gaussianity, and to some extent, violation of SI [Larson & Wandelt 2004].

¹E-mail:tarun@iucaa.ernet.in

²E-mail:amir@iucaa.ernet.in

However, what is missing is a common, well defined, mathematical language to quantify SI (as distinct from non Gaussianity) and the ability to ascribe statistical significance to the anomalies unambiguously.

Since the observed CMB sky is a single realization of the underlying correlation, the detection of SI violation or correlation patterns pose a great observational challenge. For statistically isotropic CMB sky, the correlation function

$$C(\hat{n}_1, \hat{n}_2) \equiv C(\hat{n}_1 \cdot \hat{n}_2) = \frac{1}{8\pi^2} \int d\mathcal{R} C(\mathcal{R}\hat{n}_1, \mathcal{R}\hat{n}_2), \quad (1)$$

where $\mathcal{R}\hat{n}$ denotes the direction obtained under the action of a rotation \mathcal{R} on \hat{n} , and $d\mathcal{R}$ is a volume element of the three-dimensional rotation group. The invariance of the underlying statistics under rotation allows the estimation of $C(\hat{n}_1 \cdot \hat{n}_2)$ using the average of the temperature product $\widetilde{\Delta T}(\hat{n})\widetilde{\Delta T}(\hat{n}')$ between all pairs of pixels with the angular separation θ . In the absence of statistical isotropy, $C(\hat{n}, \hat{n}')$ is estimated by a single product $\widetilde{\Delta T}(\hat{n})\widetilde{\Delta T}(\hat{n}')$ and hence is poorly determined from a single realization. Although it is not possible to estimate each element of the full correlation function $C(\hat{n}, \hat{n}')$, some measures of statistical anisotropy of the CMB map can be estimated through suitably weighted angular averages of $\widetilde{\Delta T}(\hat{n})\widetilde{\Delta T}(\hat{n}')$. The angular averaging procedure should be such that the measure involves averaging over sufficient number of independent ‘measurements’, but should ensure that the averaging does not erase all the signature of statistical anisotropy (as would happen in eq. (1) or eq. (21)). Recently, we proposed the Bipolar Power spectrum (BiPS) κ_ℓ ($\ell = 1, 2, 3, \dots$) of the CMB map as a statistical tool of detecting and measuring departure from SI [Hajian & Souradeep 2003b, Souradeep & Hajian 2003] and reviewed in this article in sec. 3. The non-zero value of the BiPS spectrum imply the break down of statistical isotropy

$$\text{STATISTICAL ISOTROPY} \implies \kappa_\ell = 0 \quad \forall \ell \neq 0. \quad (2)$$

The BiPS is sensitive to structures and patterns in the underlying total two-point correlation function [Hajian & Souradeep 2003b, Souradeep & Hajian 2003]. The BiPS is particularly sensitive to real space correlation patterns (preferred directions, etc.) on characteristic angular scales. In harmonic space, the BiPS at multipole ℓ sums power in off-diagonal elements of the covariance matrix, $\langle a_{lm} a_{l'm'} \rangle$, in the same way that the ‘angular momentum’ addition of states $lm, l'm'$ have non-zero overlap with a state with angular momentum $|l - l'| < \ell < l + l'$. Signatures, like a_{lm} and a_{l+nm} being correlated over a significant range l are ideal targets for BiPS. These are typical of SI violation due to cosmic topology and the predicted BiPS in these models have a strong spectral signature in the bipolar multipole ℓ space [Hajian & Souradeep 2003a]. The orientation independence of BiPS is an advantage since one can obtain constraints on cosmic topology that do not depend on the unknown specific orientation of the pattern (*e.g.*, preferred directions).

The results of WMAP are a milestone in CMB anisotropy measurements since it combines high angular resolution, high sensitivity, with ‘full’ sky coverage allowed by a space mission. The frequency coverage allows for WMAP CMB sky maps to be foreground cleaned up to $l \sim 100$ [Tegmark et al. 2004]. The CMB anisotropy map based on the WMAP data are ideal for testing for statistical isotropy.

2 Sources of Statistical Isotropy violation

An observed map of CMB anisotropy, ΔT_i^{obs} , contains the true CMB temperature fluctuations, ΔT_i , convolved with the beam and buried into noise and foreground contaminations. The observed map ΔT is related to the true map through this relation

$$\Delta T_i^{obs} = \sum_j B_{ij} \Delta T_j + N_i, \quad (3)$$

in which B is a matrix that contains the information about the beam smoothing effect and \mathbf{n} is the contribution from instrumental noise and foreground contamination. Hence, the observed map is a realization of a Gaussian process with covariance $C = C^T + C^N + C^{res}$ where C^T is the theoretical covariance of the CMB temperature fluctuations, C^N is the noise covariance matrix and C^{res} is the covariance of residuals of foregrounds. Breakdown of statistical isotropy $C(\hat{n}, \hat{n}') \neq C(\hat{n} \cdot \hat{n}')$ can occur in any of these parts of the correlation function. Broadly, these effects may be divided into two kinds:

- Theoretical signals: These effects are theoretically motivated and are intrinsic to the true CMB sky, ΔT . We discuss two examples of these effects, *i.e.* non-trivial cosmic topology and primordial magnetic fields, in the next subsections.
- Observational artifacts: In an ideally cleaned CMB map, the true CMB temperature fluctuations are completely extracted from the observed map. But this is not always true. Sometimes there are some artifacts (related to B or N) left in the cleaned map which may in principle violate the SI. These effects are explained in section 2.3.

2.1 Cosmic Topology & Ultra-large scale structure

The cosmic microwave background anisotropy is currently the most promising observational probe of the global spatial structure of the universe on length scales near to and even somewhat beyond the ‘horizon’ scale ($\sim cH_0^{-1}$). Figure 1 depicts a prevalent view within the concept of inflation, that this relatively smooth Hubble volume that we observe is perhaps a tiny patch of an extremely inhomogeneous and complex spatial manifold. The complexity could involve non-trivial topology (multiple connectivity) on these ultra-large scales. Within a general program to address the observability of such a diverse global structure, a more well defined and tractable path would be to restrict oneself to spaces of uniform curvature (locally homogeneous and isotropic FRW models) but with non-trivial topology; in particular, compact spaces which have additional theoretical.

The question of size and the shape of our universe are very old problems studied earlier [Ellis 1971, Sokolov & Shvartsman 1974, 1, Lachieze-Rey & Luminet 1995]. With remarkable improvements in cosmological observations, in particular the CMB anisotropy measurements, these questions have received considerable attention over the past few years [de Oliveira-Costa et al. 1996, Starkman 1998, Levin et al. 1998, Bond, Pogosyan & Souradeep 1998, 2000, de Oliveira-Costa et al. 2003, Dineen et al. 2004, Copi et al. 2004]. Although a multiply connected universe sounds non-trivial, but there are theoretical motivations [Linde 2004, Levin 2002] to favor a spatially compact universe. One possibility to have a compact flat universe is the consideration of multiply connected (topologically nontrivial) spaces. The oldest way of searching for global structure of the universe is by identifying ghost images of local galaxies and clusters or quasars at higher redshifts [Lachieze-Rey & Luminet 1995]. This method can probe the topology of the universe only on scales substantially smaller than the apparent radius of the observable universe. Another method to search for the shape of the universe is through the effect on the cosmic density perturbation fields. For compact topologies, the two main effects on the CMB are: (1) the breaking of statistical isotropy in characteristic patterns determined by the photon geodesic structure of the manifold and (2) an infrared cutoff in the power spectrum of perturbations imposed by the finite spatial extent. More generally, in a universe with non-trivial global spatial topology, the multiple connectivity of the space could lead to observable characteristic angular correlation patterns in the CMB anisotropy.

Over the past few years, many independent methods have been proposed to search for evidence of a finite universe in CMB maps. These methods can be classified in three main groups.

- Using the angular power spectrum of CMB anisotropies to probe the topology of the Universe. The angular power spectrum, however, is inadequate to characterize the peculiar form of the anisotropy manifest in small universes of this type. Since nontrivial topology breaks down SI, there is more information in a map of temperature fluctuations than just the angular power spectrum [Levin et al. 1998, Bond, Pogosyan & Souradeep 1998, 2000, Hajian & Souradeep 2003a].
- The second class of methods are direct methods that rely on multiple imaging (or strong correlation features) of the CMB sky. The most well known methods among these methods are S-map statistics [de Oliveira-Costa et al. 1996, de Oliveira-Costa et al. 2003] and the search for circles-in-the-sky [Cornish, Spergel & Starkman 1998].
- Third class of methods are indirect probes which deal with the correlation patterns of the CMB anisotropy field by using an appropriate combination of coefficients of the harmonic expansion of the field [Dineen et al. 2004, Donoghue et al. 2004, Hajian & Souradeep 2003a, Copi et al. 2004]. The Bipolar power spectrum (BiPS) method is one of the strategies in this class.

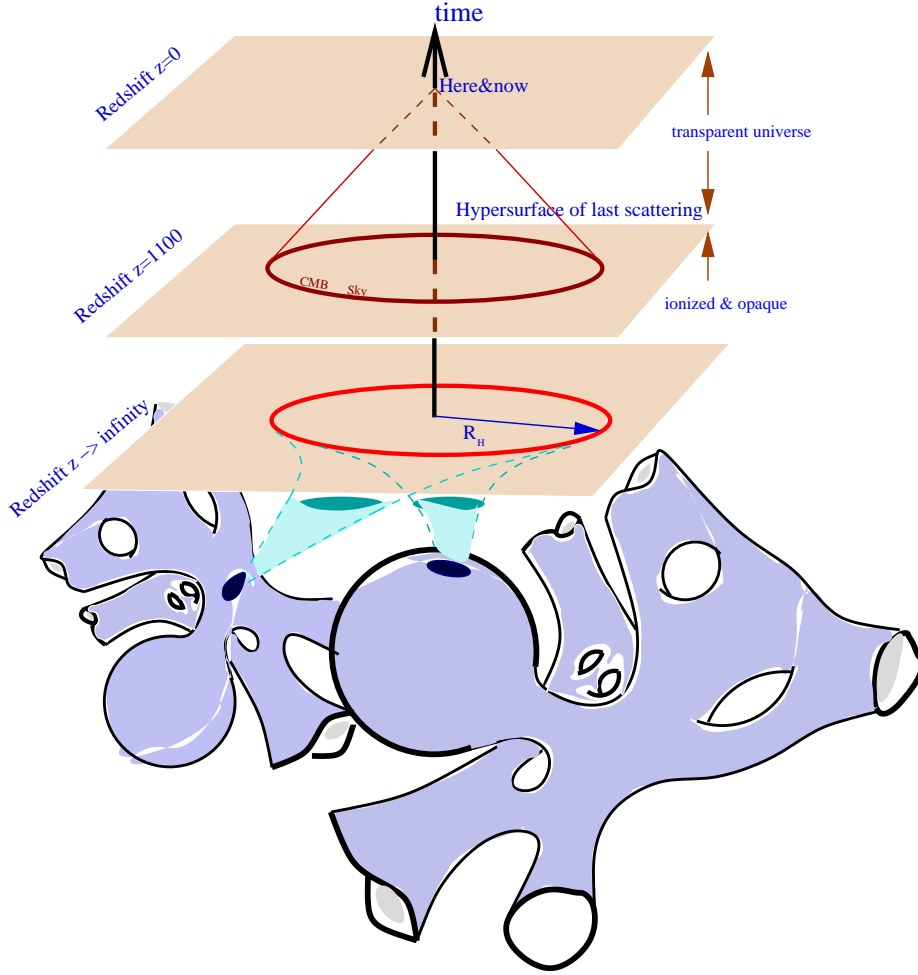


Figure 1: A cartoon depicting a prevalent view within the inflationary paradigm. The observable universe corresponds to a small patch of a very complicated manifold that has been blown to cosmological scales during an inflationary epoch. Ultra-large scale structure could be observable if the size of this patch is not much smaller than the scales of inhomogeneity and non-trivial topology.

The correlation patterns in CMB that lead to violation of SI implies that $\langle \hat{a}_{lm} \hat{a}_{lm}^* \rangle$ has off-diagonal elements. Figure 2 taken from [Bond, Pogosyan & Souradeep 1998, 2000] shows the off-diagonal elements in the CMB correlation for two compact universe models. BiPS gathers together the power in the off-diagonal elements of $\langle \hat{a}_{lm} \hat{a}_{lm}^* \rangle$ as shown in Fig. 3.

Using the fact that statistical isotropy is violated in compact spaces one could use the bipolar power spectrum as a probe to detect the topology of the universe. A simple example of is the BiPS signature of a non-trivial topology can be given for a T^3 universe, where the correlation function is given by

$$C(\hat{q}, \hat{q}') = L^{-3} \sum_{\mathbf{n}} P_{\Phi}(k_{\mathbf{n}}) e^{-i\pi(\epsilon_{\hat{q}} \mathbf{n} \cdot \hat{q} - \epsilon_{\hat{q}'} \mathbf{n} \cdot \hat{q}')}, \quad (4)$$

in which, \mathbf{n} is 3-tuple of integers (in order to avoid confusion, we use \hat{q} to represent the direction instead of \hat{n}), the small parameter $\epsilon_{\hat{q}} \leq 1$ is the physical distance to the SLS along \hat{q} in units of $L/2$ (more generally, $\bar{L}/2$ where $\bar{L} = (L_1 L_2 L_3)^{1/3}$) and L is the size of the Dirichlet domain (DD). When ϵ is a small constant, the leading order terms in the correlation function eq. (4) can be readily obtained in power

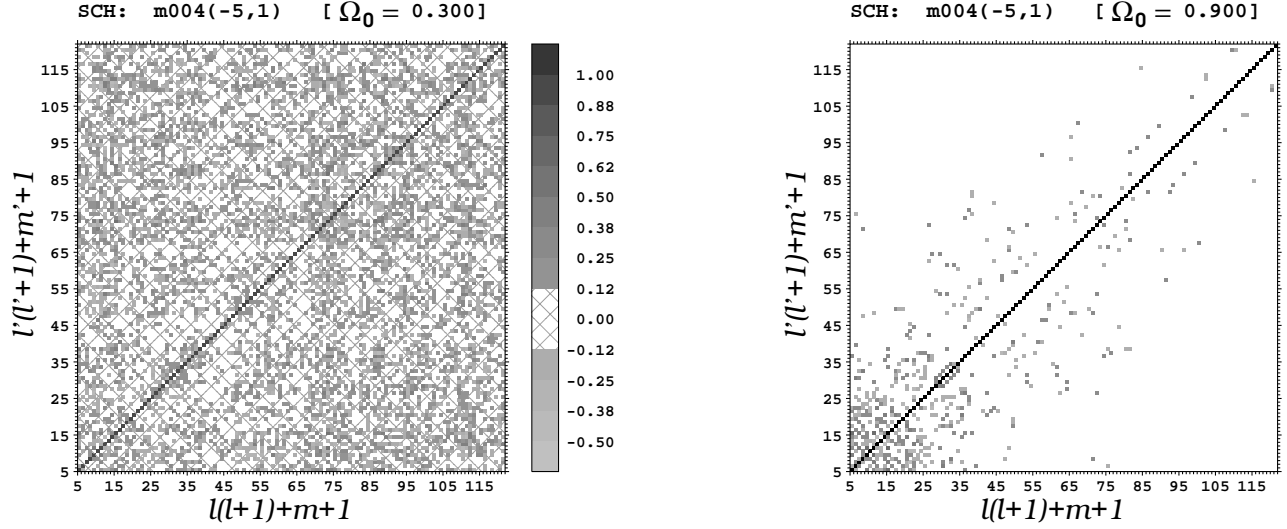


Figure 2: The figure taken from [Bond,Pogosyan & Souradeep 1998,2000] illustrates the non-diagonal nature of the expectation values of $a_{\ell m}$ pair products when the CMB anisotropy violates SI in two model compact universe. The radical violation in the model on the left corresponds to a small compact universe where CMB photons have traversed across multiple times. The model on the right with mild violation of SI corresponds to a universe of size comparable to the observable horizon. For more details, see [Bond,Pogosyan & Souradeep 1998,2000]

series expansion in powers of ϵ . For the lowest wave numbers $|\mathbf{n}|^2 = 1$ in a cuboid torus

$$\begin{aligned}
 C(\hat{q}, \hat{q}') &\approx 2 \sum_i P_{\Phi}(2\pi/L_i) \cos(\pi\epsilon\beta_i\Delta q_i) \\
 &\approx C_0 \left[1 - \epsilon^2 |\Delta q|^2 + 3\epsilon^4 \sum_{i=1}^3 (\Delta q_i)^4 \right],
 \end{aligned} \tag{5}$$

where Δq_i are the components of $\Delta \mathbf{q} = \hat{q} - \hat{q}'$ along the three axes of the torus and $\beta_i = \bar{L}/L_i$. From this, the non-zero κ_{ℓ} can be analytically computed to be

$$\begin{aligned}
 \frac{\kappa_0}{C_0^2} &= \pi^2(1 - 4\epsilon^2 + \frac{368}{15}\epsilon^4 - \frac{288}{5}\epsilon^6 + \frac{20736}{125}\epsilon^8) \\
 \frac{\kappa_4}{C_0^2} &= \frac{12288\pi^2}{875}\epsilon^8
 \end{aligned} \tag{6}$$

κ_4 has the information of the relative size of the Dirichlet domain and one can use it to constrain the topology of the universe. A detailed study of the BiPS signature of cosmic topology is given in [Hajian & Souradeep 2003a]. These prediction allow us to constrain cosmic topology using the BiPS measured in the observed CMB maps [Hajian et al. 2004].

2.2 Primordial Magnetic Fields

Cosmological magnetic field, generated during an early epoch of inflation [Ratra 1992, Bamba et al. 2004], can generate CMB anisotropies [Durrer et al. 1998]. The presence of a preferred direction due to a homogeneous magnetic field background leads to non-zero off-diagonal elements in the covariance matrix [Chen et al. 2004]. This induces correlations between $a_{l+1,m}$ and $a_{l-1,m}$ multipole coefficients of the CMB temperature anisotropy field in the following manner

$$\langle a_{lm} a_{l'm'}^* \rangle = \delta_{m,m'} [\delta_{l,l'} C_l + (\delta_{l+1,l'-1} + \delta_{l-1,l'+1} D_l)], \tag{7}$$

where D_l is the power spectrum of off-diagonal elements of the covariance matrix. For a Harrison-Peebles-Yu-Zel'dovich scale-invariant spectrum, D_l behaves as l^{-2} . More precisely, it is given by

$$D_l = 4 \times 10^{-16} l^{-2} \left(\frac{B}{1nG}\right)^4. \quad (8)$$

This clearly violates the statistical isotropy and gives rise to a non-zero BiPS predictions for magnetic fields. This opens the way to use BiPS analysis on CMB maps to constrain or measure primordial cosmic magnetic fields [Hajian et al. 2004b].

2.3 Observational Artifacts

Foregrounds and observational artifacts (such as non-circular beam, incomplete/non-uniform sky coverage and anisotropic noise) would also manifest themselves as violations of SI.

- **Anisotropic noise** : The CMB temperature measured by an instrument is a linear sum of the cosmological signal as well as instrumental noise. The two point correlation function then has two parts, one part comes from the signal and the other one comes from the noise

$$C(\hat{n}_1, \hat{n}_2) = C^S(\hat{n}_1, \hat{n}_2) + C^N(\hat{n}_1, \hat{n}_2). \quad (9)$$

Both signal and noise should be statistically isotropic to have a statistically isotropic CMB map. So even for a statistically isotropic signal, if the noise fails to be statistically isotropic the resultant map will turn out to be anisotropic. The noise matrix can fail to be statistically isotropic due to non-uniform coverage. Also if the noise is correlated between different pixels the noise matrix could be statistically anisotropic. A simple example of this is the diagonal (but anisotropic) noise given by the following correlation

$$C^N(\hat{n}, \hat{n}') = \sigma^2(\hat{n})\delta_{\hat{n}\hat{n}'}. \quad (10)$$

This noise clearly violates the SI and will lead to a non-zero BiPS given by

$$\kappa_\ell = \sum_{m=-\ell}^{\ell} |f_{\ell m}|^2, \quad (11)$$

where $f_{\ell m}$ are spherical harmonic transform of the noise, $f_{\ell m} = \int d\Omega_{\hat{n}} Y_{\ell m}^*(\hat{n})\sigma^2(\hat{n})$.

- **The effect of non-circular beam** : In practice when we deal with data, it is necessary to take into account the *instrumental response*. The instrumental response is nothing but the beams width and the form of the beam and can be taken into account by defining a beam profile function $B(\hat{n}, \hat{n}')$. Here \hat{n} denotes the direction to the center of the beam and \hat{n}' denotes the direction of the incoming photon. The temperature measured by the instrument is given by

$$\Delta\tilde{T}(\hat{n}) = \int \Delta T(\hat{n}')B(\hat{n}, \hat{n}')d\Omega_{\hat{n}'}. \quad (12)$$

Using this relation to calculate the correlation function $\tilde{C}(\hat{n}_1, \hat{n}_2) = \langle \Delta\tilde{T}(\hat{n}_1)\Delta\tilde{T}(\hat{n}_2) \rangle$ one would get

$$\begin{aligned} \tilde{C}(\hat{n}_1, \hat{n}_2) &= \int d\Omega_{\hat{n}'} \int d\Omega_{\hat{n}''} \langle \Delta T(\hat{n}')\Delta T(\hat{n}'') \rangle B(\hat{n}_1, \hat{n}')B(\hat{n}_2, \hat{n}'') \\ &= \int d\Omega_{\hat{n}'} \int d\Omega_{\hat{n}''} C(\hat{n}', \hat{n}'')B(\hat{n}_1, \hat{n}')B(\hat{n}_2, \hat{n}''). \end{aligned} \quad (13)$$

Only for a circular beam where $B(\hat{n}, \hat{n}') \equiv B(\hat{n} \cdot \hat{n}')$, the correlation function is statistically isotropic, $\tilde{C}(\hat{n}_1, \hat{n}_2) \equiv \tilde{C}(\hat{n}_1 \cdot \hat{n}_2)$. Breakdown of SI is obvious since even C_l get mixed for a non-circular beam, $\tilde{C}_l = \sum_{l'} A_{ll'}C_{l'}$ [Mitra et al. 2004]. Non-circularity of the beam in CMB anisotropy experiments is becoming increasingly important as experiments go for higher resolution measurements at higher sensitivity.

- **Mask effects** : Many experiments map only a part of the sky. Even in the best case, contamination by galactic foreground residuals make parts of the sky unusable. The incomplete sky or mask effect is another source of breakdown of SI. But, this effect can be readily modeled out. The effect of a general mask on the temperature field is as follows

$$\Delta T^{masked}(\hat{n}) = \Delta T(\hat{n})W(\hat{n}), \quad (14)$$

where $W(\hat{n})$ is the mask function. One can cut different parts of the sky by choosing appropriate mask functions. Masked a_{lm} coefficients can be computed from the masked temperature field,

$$\begin{aligned} a_{lm}^{masked} &= \int \Delta T^{masked}(\hat{n}) Y_{lm}^*(\hat{n}) d\Omega_{\hat{n}} \\ &= \sum_{l_1 m_1} a_{l_1 m_1} \int Y_{l_1 m_1}(\hat{n}) Y_{lm}^*(\hat{n}) W(\hat{n}) d\Omega_{\hat{n}}. \end{aligned} \quad (15)$$

Where $a_{l_1 m_1}$ are spherical harmonic transforms of the original temperature field. We can expand $W(\hat{n})$ in spherical harmonics as well

$$W(\hat{n}) = \sum_{lm} w_{lm} Y_{lm}(\hat{n}), \quad (16)$$

and after substituting this into eq. (15) it is seen that the masked a_{lm} is given by the effect of a kernel $K_{lm}^{l_1 m_1}$ on original $a_{l_1 m_1}$ [Prunet et al. 2004]

$$a_{lm}^{masked} = \sum_{l_1 m_1} a_{l_1 m_1} K_{lm}^{l_1 m_1}. \quad (17)$$

The kernel contains the information of our mask function and is defined by

$$\begin{aligned} K_{lm}^{l_1 m_1} &= \sum_{l_2 m_2} w_{l_2 m_2} \int Y_{l_1 m_1}(\hat{n}) Y_{l_2 m_2}(\hat{n}) Y_{lm}^*(\hat{n}) d\Omega_{\hat{n}} \\ &= \sum_{l_2 m_2} w_{l_2 m_2} \sqrt{\frac{(2l_1 + 1)(2l_2 + 1)}{4\pi(2l + 1)}} C_{l_1 0 l_2 0}^{l 0} C_{l_1 m_1 l_2 m_2}^{lm}. \end{aligned} \quad (18)$$

The covariance matrix of a masked sky will no longer have the diagonal form because of the action of the kernel

$$\begin{aligned} \langle a_{lm}^{masked} a_{l'm'}^{masked*} \rangle &= \langle a_{l_1 m_1} a_{l'_1 m'_1}^* \rangle K_{lm}^{l_1 m_1} K_{l'm'}^{l'_1 m'_1} \\ &= C_{l_1} \delta_{l_1 l'_1} \delta_{m_1 m'_1} K_{lm}^{l_1 m_1} K_{l'm'}^{l'_1 m'_1} \\ &= \sum_{l_1, m_1} C_{l_1} K_{lm}^{l_1 m_1} K_{l'm'}^{l_1 m_1}. \end{aligned} \quad (19)$$

This clearly violates the SI and results a non-zero BiPS for masked CMB skies. In the next section we apply a galactic mask to ILC map and show that signature of this mask on BiPS is a rising tail at low ℓ , ($\ell < 20$).

- **Residuals from foreground removal** : Besides the cosmological signal and instrumental noise, a CMB map also contains foreground emission such as galactic emission, etc. The foreground is usually modeled out using spectral information. However, residuals from foreground subtractions in the CMB map will violate SI. Interestingly, BiPS does sense the difference between maps with grossly different emphasis on the galactic foreground. As shown in [Hajian & Souradeep 2005b] the BiPS of a Wiener filtered map shows a signal very similar to that of a galactic cut sky. This can be understood if one writes the effect of the Wiener filter as a weight on the ‘contaminated’ galactic regions of the map.

$$\Delta T^W(\hat{n}) = \Delta T(\hat{n})(1 + W(\hat{n})). \quad (20)$$

This explains the similarity between a cut sky and a Wiener filtered map. The effect of foregrounds on BiPS still needs to be studied more carefully.

3 The Bipolar Power Spectrum (BiPS)

Two point correlation of the CMB anisotropy is given by ensemble average, but there is only one observable CMB sky. Hence, the ensemble average is meaningless unless the CMB sky is SI, when the two point correlation function $C(\theta)$ can be well estimated as in eq. (21) by the average product of temperature fluctuations over all pairs of directions \hat{n}_1 and \hat{n}_2 whose angular separation is θ . In particular, for CMB temperature map $\widetilde{\Delta T}(\hat{n}_i)$ defined on a discrete set of points on celestial sphere (pixels) \hat{n}_i ($i = 1, \dots, N_p$)

$$\tilde{C}(\theta) = \sum_{i,j=1}^{N_p} \widetilde{\Delta T}(\hat{n}_i) \widetilde{\Delta T}(\hat{n}_j) \delta(\cos \theta - \hat{n}_i \cdot \hat{n}_j), \quad (21)$$

is an estimator of the correlation function $C(\theta)$ of an underlying SI statistics. If the statistical isotropy is violated the estimate of the correlation function from a sky map given by a single temperature product

$$\tilde{C}(\hat{n}_1, \hat{n}_2) = \Delta T(\hat{n}_1) \Delta T(\hat{n}_2) \quad (22)$$

is poorly determined.

Although it is not possible to estimate each element of the full correlation function $C(\hat{n}_1, \hat{n}_2)$, some measures of statistical isotropy of the CMB map can be estimated through suitably weighted angular averages of $\Delta T(\hat{n}_1) \Delta T(\hat{n}_2)$. The angular averaging procedure should be such that the measure involves averaging over sufficient number of independent measurements, but should ensure that the averaging does not erase all the signature of statistical anisotropy. Another important desirable property is that measure be independent of the overall orientation of the sky. Based on these considerations, we have proposed a set of measures of statistical isotropy [Hajian & Souradeep 2003b]

$$\kappa^\ell = (2\ell + 1)^2 \int d\Omega_{n_1} \int d\Omega_{n_2} \left[\frac{1}{8\pi^2} \int d\mathcal{R} \chi^\ell(\mathcal{R}) C(\mathcal{R}\hat{n}_1, \mathcal{R}\hat{n}_2) \right]^2. \quad (23)$$

In the above expression, $C(\mathcal{R}\hat{n}_1, \mathcal{R}\hat{n}_2)$ is the two point correlation at $\mathcal{R}\hat{n}_1$ and $\mathcal{R}\hat{n}_2$ which are the coordinates of the two pixels \hat{n}_1 and \hat{n}_2 after rotating the coordinate system through an angle ω where ($0 \leq \omega \leq \pi$) about the axis $\mathbf{n}(\Theta, \Phi)$. The direction of this rotation axis \mathbf{n} is defined by the polar angles Θ where ($0 \leq \Theta \leq \pi$) and Φ , where ($0 \leq \Phi \leq 2\pi$). χ^ℓ is the trace of the finite rotation matrix in the ℓM -representation

$$\chi^\ell(\mathcal{R}) = \sum_{M=-\ell}^{\ell} D_{MM}^\ell(\mathcal{R}), \quad (24)$$

which is called the *characteristic function*, or the character of the irreducible representation of rank ℓ . It is invariant under rotations of the coordinate systems. Explicit forms of $\chi^\ell(\mathcal{R})$ are simple when \mathcal{R} is specified by ω, Θ, Φ , then $\chi^\ell(\mathcal{R})$ is completely determined by the rotation angle ω and it is independent of the rotation axis $\mathbf{n}(\Theta, \Phi)$,

$$\begin{aligned} \chi^\ell(\mathcal{R}) &= \chi^\ell(\omega) \\ &= \frac{\sin [(2\ell + 1)\omega/2]}{\sin [\omega/2]}. \end{aligned} \quad (25)$$

And finally $d\mathcal{R}$ in eq.(23) is the volume element of the three-dimensional rotation group and is given by

$$d\mathcal{R} = 4 \sin^2 \frac{\omega}{2} d\omega \sin \Theta d\Theta d\Phi. \quad (26)$$

For a statistically isotropic model $C(\hat{n}_1, \hat{n}_2)$ is invariant under rotation, and therefore $C(\mathcal{R}\hat{n}_1, \mathcal{R}\hat{n}_2) = C(\hat{n}_1, \hat{n}_2)$ and the orthonormality of $\chi^\ell(\omega)$, we will recover the condition for SI,

$$\kappa^\ell = \kappa^0 \delta_{\ell 0}. \quad (27)$$

Real-space representation of BiPS is very suitable for analytical computation of BiPS for theoretical models where we know the analytical expression for the two point correlation of the model, such as

theoretical models in [Hajian & Souradeep 2003a]. On the other hand, the harmonic representation of BiPS that we describe next allows computationally rapid methods for BiPS estimation from a given CMB map.

Two point correlation of CMB anisotropies, $C(\hat{n}_1, \hat{n}_2)$, is a two point function on $S^2 \times S^2$, and hence can be expanded as

$$C(\hat{n}_1, \hat{n}_2) = \sum_{l_1, l_2, L, M} A_{l_1 l_2}^{\ell M} \{Y_{l_1}(\hat{n}_1) \otimes Y_{l_2}(\hat{n}_2)\}_{\ell M}, \quad (28)$$

where $A_{l_1 l_2}^{\ell M}$ are coefficients of the expansion (here after BipoSH coefficients) and $\{Y_{l_1}(\hat{n}_1) \otimes Y_{l_2}(\hat{n}_2)\}_{\ell M}$ are the bipolar spherical harmonics which transform as a spherical harmonic with ℓ, M with respect to rotations [Varshalovich et al. 1988] given by

$$\{Y_{l_1}(\hat{n}_1) \otimes Y_{l_2}(\hat{n}_2)\}_{\ell M} = \sum_{m_1 m_2} C_{l_1 m_1 l_2 m_2}^{\ell M} Y_{l_1 m_1}(\hat{n}_2) Y_{l_2 m_2}(\hat{n}_2), \quad (29)$$

in which $C_{l_1 m_1 l_2 m_2}^{\ell M}$ are Clebsch-Gordan coefficients. We can inverse-transform $C(\hat{n}_1, \hat{n}_2)$ to get the $A_{l_1 l_2}^{\ell M}$ by multiplying both sides of eq.(28) by $\{Y_{l_1}(\hat{n}_1) \otimes Y_{l_2}(\hat{n}_2)\}_{\ell' M'}^*$ and integrating over all angles, then the orthonormality of bipolar harmonics implies that

$$A_{l_1 l_2}^{\ell M} = \int d\Omega_{\hat{n}_1} \int d\Omega_{\hat{n}_2} C(\hat{n}_1, \hat{n}_2) \{Y_{l_1}(\hat{n}_1) \otimes Y_{l_2}(\hat{n}_2)\}_{\ell M}^*. \quad (30)$$

The above expression and the fact that $C(\hat{n}_1, \hat{n}_2)$ is symmetric under the exchange of \hat{n}_1 and \hat{n}_2 lead to the following symmetries of $A_{l_1 l_2}^{\ell M}$

$$\begin{aligned} A_{l_2 l_1}^{\ell M} &= (-1)^{(l_1 + l_2 - L)} A_{l_1 l_2}^{\ell M}, \\ A_{l l}^{\ell M} &= A_{l l}^{\ell M} \delta_{\ell, 2k+1}, \quad k = 0, 1, 2, \dots \end{aligned} \quad (31)$$

The Bipolar Spherical Harmonic (BipoSH) coefficients, $A_{l_1 l_2}^{\ell M}$, are linear combinations of off-diagonal elements of the covariance matrix,

$$A_{l_1 l_2}^{\ell M} = \sum_{m_1 m_2} \langle a_{l_1 m_1} a_{l_2 m_2}^* \rangle (-1)^{m_2} C_{l_1 m_1 l_2 - m_2}^{\ell M}. \quad (32)$$

This means that $A_{l_1 l_2}^{\ell M}$ completely represent the information of the covariance matrix. Fig. 3 shows how $A_{l_1 l_2}^{2M}$ and $A_{l_1 l_2}^{4M}$ combine the elements of the covariance matrix. When SI holds, the covariance matrix is diagonal and hence

$$\begin{aligned} A_{l l'}^{\ell M} &= (-1)^l C_l (2l+1)^{1/2} \delta_{l l'} \delta_{\ell 0} \delta_{M 0}, \\ A_{l_1 l_2}^{00} &= (-1)^{l_1} \sqrt{2l_1 + 1} C_{l_1} \delta_{l_1 l_2}. \end{aligned} \quad (33)$$

BipoSH expansion is the most general representation of the two point correlation functions of CMB anisotropy. The well known angular power spectrum, C_l is a subspace of BipoSH coefficients corresponding to the $A_{l l}^{00}$ that represent the statistically isotropic part of a general correlation function. When SI holds, $A_{l l}^{00}$ or equivalently C_l have all the information of the field. But if the SI breaks down, $A_{l l}^{00}$ are not adequate for describing the field, and one needs to take the other terms into account. This simply means that the And when the statistical isotropy holds, these coefficients will reduce to the well-known angular power spectrum of CMB anisotropy.

It is impossible to measure all $A_{l_1 l_2}^{\ell M}$ individually because of cosmic variance. Combining BipoSH coefficients into Bipolar Power Spectrum reduces the cosmic variance³. BiPS of CMB anisotropy is defined as a convenient contraction of the BipoSH coefficients

$$\kappa_\ell = \sum_{l, l', M} |A_{l l'}^{\ell M}|^2 \geq 0. \quad (34)$$

³This is similar to combining a_{lm} to construct the angular power spectrum, $C_l = \frac{1}{2l+1} \sum_m |a_{lm}|^2$, to reduce the cosmic variance

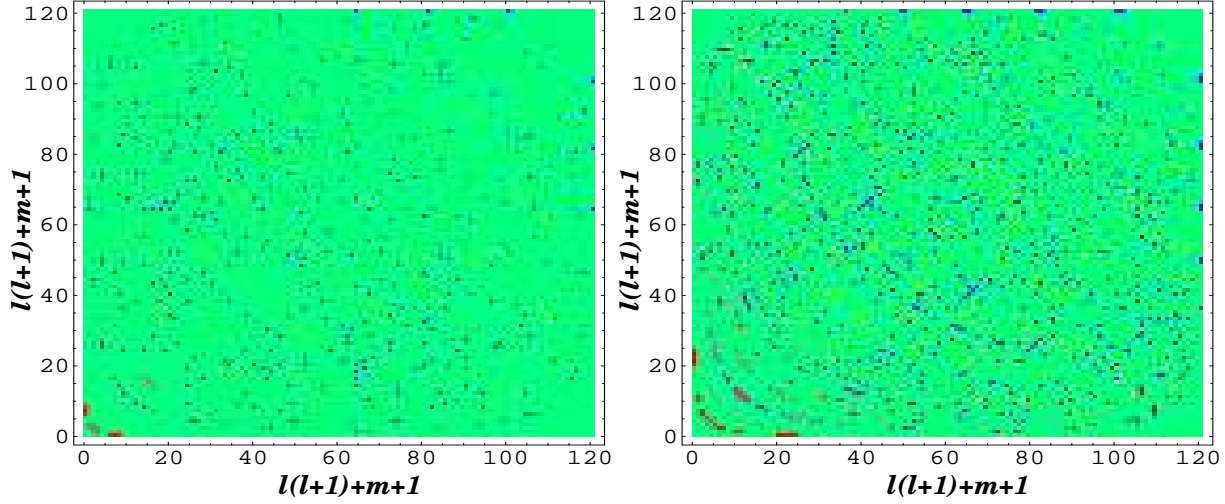


Figure 3: BiPSH coefficients are linear combinations of elements of the covariance matrix. Here $A_{ll'}^{2M}$ (left) and $A_{ll'}^{4M}$ (right) are plotted to show how BiPS covers the off-diagonal elements of the covariance matrix in harmonic space.

The BiPS, which can be shown that is equivalent to the one in eq.(23), has interesting properties. It is orientation independent and is invariant under rotations of the sky. For models in which statistical isotropy is valid, BiPSH coefficients are given by eq. (33). And results in a null BiPS, *i.e.* $\kappa_\ell = 0$ for every positive ℓ ,

$$\kappa_\ell = \kappa_0 \delta_{\ell 0}. \quad (35)$$

3.1 Unbiased Estimator of BiPS

An estimator for measuring BiPSH coefficients from a given CMB map is

$$\tilde{A}_{ll'}^{\ell M} = \sum_{mm'} \sqrt{W_l W_{l'}} a_{lm} a_{l'm'} C_{lml'm'}^{\ell M}, \quad (36)$$

where W_l is the Legendre transform of the window function. The above estimator is a linear combination of C_l and hence is unbiased. An unbiased estimator of BiPS is given by

$$\tilde{\kappa}_\ell = \sum_{ll'M} \left| \tilde{A}_{ll'}^{\ell M} \right|^2 - \mathfrak{B}_\ell, \quad (37)$$

where the bias for the BiPS is defined as $\mathfrak{B}_\ell = \langle \tilde{\kappa}_\ell \rangle - \kappa_\ell$ is equal to

$$\begin{aligned} \mathfrak{B}_\ell = & \sum_{l_1, l_2} W_{l_1} W_{l_2} \sum_{m_1, m'_1} \sum_{m_2, m'_2} \left[\langle a_{l_1 m_1}^* a_{l_1 m'_1} \rangle \langle a_{l_2 m_2}^* a_{l_2 m'_2} \rangle + \langle a_{l_1 m_1}^* a_{l_2 m'_2} \rangle \langle a_{l_2 m_2}^* a_{l_1 m'_1} \rangle \right] \\ & \times \sum_M C_{l_1 m_1 l_2 m_2}^{\ell M} C_{l_1 m'_1 l_2 m'_2}^{\ell M}. \end{aligned} \quad (38)$$

The above expression for \mathfrak{B}_ℓ is obtained by assuming Gaussian statistics of the temperature fluctuations. The procedure is very similar to computing cosmic variance (which is discussed in the next section), but much simpler. However, we can not measure the ensemble average in the above expression and as a result, elements of the covariance matrix (obtained from a single map) are poorly determined due to the cosmic variance. The best we can do is to compute the bias for the SI component of a map

$$\mathfrak{B}_\ell \equiv \langle \tilde{\kappa}_\ell^B \rangle_{\text{SI}} = (2\ell + 1) \sum_{l_1} \sum_{l_2=|\ell-l_1|}^{\ell+l_1} C_{l_1} C_{l_2} W_{l_1} W_{l_2} [1 + (-1)^\ell \delta_{l_1 l_2}]. \quad (39)$$

Note, the estimator $\tilde{\kappa}_\ell$ is unbiased, only for SI correlation, i.e., $\langle \tilde{\kappa}_\ell \rangle = 0$. Consequently, for SI correlation, the measured $\tilde{\kappa}_\ell$ will be consistent with zero within the error bars given by σ_{SI} [Hajian & Souradeep 2003b]. We simulated 1000 SI CMB maps and computed BiPS for them using different filters. The average BiPS of SI maps is an estimation of the bias which can be compared to our analytical estimation. The left panel of Fig. 4 shows that the theoretical bias (computed from average C_l) match the numerical estimations of average κ_ℓ of the 1000 realizations of the SI maps.

It is important to note that bias cannot be correctly subtracted for non-SI maps. Non-zero $\tilde{\kappa}_\ell$ estimated from a non-SI map will have contribution from the non-SI terms in full bias given in eq. (38). It is not inconceivable that for strong SI violation, \mathfrak{B}_ℓ over-corrects for the bias leading to negative values of $\tilde{\kappa}_\ell$. What is important is whether measured $\tilde{\kappa}_\ell$ differs from zero at a statistically significant level.

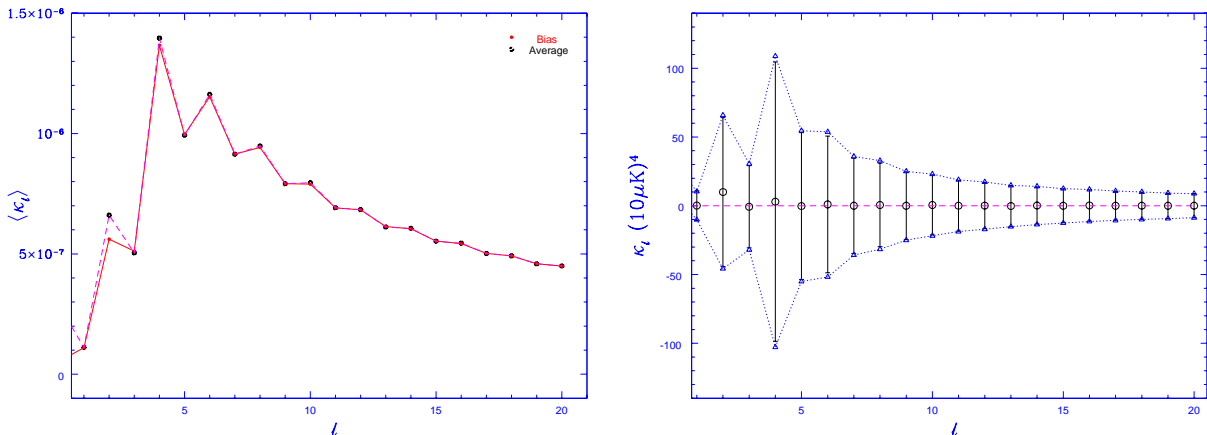


Figure 4: **Left:** Analytical bias for a Gaussian window function with $W_l^G(40)$ computed from the average C_l from 1000 realizations of a SI CMB map compared with $\langle \kappa_l^{realization} \rangle$ (the average κ_l from 1000 realizations). This shows that the theoretical bias is a very good estimation of the bias for a statistically isotropic map. **Right:** The cosmic error, $\sigma(\kappa_\ell)$, obtained using 1000 independent realizations of CMB (full) sky map matches the analytical results shown by dotted curve with triangles. This shows a much better fit to the theoretical cosmic variance compared to what was obtained for 100 realizations [Hajian & Souradeep 2003b]

3.2 Cosmic Variance of BiPS

A crucial point is how well one can hope to estimate the BiPS given the single observed sky. This is limited by the Cosmic variance of the BiPS estimator defined as

$$\sigma^2 = \langle \tilde{\kappa}_\ell^2 \rangle - \langle \tilde{\kappa}_\ell \rangle^2 \quad (40)$$

It is possible to obtain an analytic expression variance of $\tilde{\kappa}^\ell$ using the Gaussianity of ΔT . Looking back at the eq.(23) we can see, we will have to calculate the eighth moment of the field

$$\langle \Delta T(\hat{n}_1) \Delta T(\hat{n}_2) \Delta T(\hat{n}_3) \Delta T(\hat{n}_4) \Delta T(\hat{n}_5) \Delta T(\hat{n}_6) \Delta T(\hat{n}_7) \Delta T(\hat{n}_8) \rangle. \quad (41)$$

Assuming Gaussianity of the field we can rewrite the eight point correlation in terms of two point correlations. One can write a simple code to do that⁴. This will give us $(8-1)!! = 7 \times 5 \times 3 = 105$ terms. These 105 terms consist of terms like:

$$\langle \Delta T(\hat{n}_1) \Delta T(\hat{n}_2) \rangle \langle \Delta T(\hat{n}_3) \Delta T(\hat{n}_4) \rangle \langle \Delta T(\hat{n}_5) \Delta T(\hat{n}_6) \rangle \langle \Delta T(\hat{n}_7) \Delta T(\hat{n}_8) \rangle, \quad (42)$$

and all other permutations of them. On the other hand $\langle \tilde{\kappa}_\ell \rangle$ has a 4 point correlation in it which can also be expanded versus two point correlation functions. If we form $\langle \tilde{\kappa}_\ell^2 \rangle - \langle \tilde{\kappa}_\ell \rangle^2$, only 96 terms will be

⁴F90 software implementing this is available from the authors upon request

left which are in the following form

$$\left(\frac{2\ell+1}{8\pi^2}\right)^2 \int d\Omega_1 \cdots d\Omega_4 \int dR \int dR' \chi_\ell(R) \chi_\ell(R') C(\hat{n}_1, R' \hat{n}_4) C(\hat{n}_2, R' \hat{n}_3) C(R \hat{n}_1, \hat{n}_4) C(R \hat{n}_2, \hat{n}_3) \quad (43)$$

and all other permutations. As described in detail in our paper [Hajian & Souradeep 2005b], it is possible to simplify and group together the 96 terms and obtain a compact expression as

$$\begin{aligned} \sigma_{\text{SI}}^2(\tilde{\kappa}_\ell) &= \sum_{l:2l \geq \ell} 4 C_l^4 W_l^4 \left[2 \frac{(2\ell+1)^2}{2l+1} + (-1)^\ell (2\ell+1) + (1+2(-1)^\ell) F_l^\ell \right] \\ &+ \sum_{l_1} \sum_{l_2=|\ell-l_1|}^{\ell+l_1} 4 C_{l_1}^2 C_{l_2}^2 W_{l_1}^2 W_{l_2}^2 [(2\ell+1) + F_{l_1 l_2}^\ell] \\ &+ 8 \sum_{l_1} \frac{(2\ell+1)^2}{2l_1+1} C_{l_1}^2 W_{l_1}^2 \left[\sum_{l_2=|\ell-l_1|}^{\ell+l_1} C_{l_2} W_{l_2} \right]^2 \\ &+ 16 (-1)^\ell \sum_{l_1:2l_1 \geq \ell} \frac{(2\ell+1)^2}{2l_1+1} \sum_{l_2=|\ell-l_1|}^{\ell+l_1} C_{l_1}^3 C_{l_2} W_{l_1}^3 W_{l_2}. \end{aligned} \quad (44)$$

Numerical computation of σ_{SI}^2 is fast. But the challenge is to compute Clebsch-Gordan coefficients for large quantum numbers. We use `drc3j` subroutine of `netlib`⁵ in order to compute the Clebsch-Gordan coefficients in our codes. Again we can check the accuracy of our analytical estimation of cosmic variance by comparing it against the standard deviation of BiPS of 1000 simulations of SI CMB sky. The result is shown the right panel of in Fig. 4 and shows a very good agreement between the two.

4 Results of BiPS analysis of WMAP CMB maps

We carry out measurement of the BiPS, on the following CMB anisotropy maps

- A) a foreground cleaned map (denoted as ‘TOH’) [Tegmark et al. 2004],
- B) the Internal Linear Combination map (denoted as ‘ILC’ in the figures) [Bennett et al. 2003], and
- C) a customized linear combination of the QVW maps of WMAP with a galactic cut (denoted as ‘CSSK’).

Also for comparison, we measure the BiPS of

- D) a Wiener filtered map of WMAP data (denoted as ‘Wiener’) [Tegmark et al. 2004], and
- E) the ILC map with a 10° cut around the equator (denoted as ‘Gal. cut.’).

Angular power spectra of these maps are shown in Fig. 5. The best fit theoretical power spectrum from the WMAP analysis⁶ [Spergel et al. 2003] is plotted on the same figure. C_l from observed maps are consistent with the theoretical curve, C_l^T (except for the lowest multipoles). The bias and cosmic variance of BiPS depend on the total SI angular power spectrum of the signal and noise $C_l = C_l^S + C_l^N$. However, we have restricted our analysis to $l \lesssim 60$ where the errors in the WMAP power spectrum is dominated by cosmic variance. It is conceivable that the SI violation is limited to particular range of angular scales. Hence, multipole space windows that weigh down the contribution from the SI region of multipole space will enhance the signal relative to cosmic error, σ_{SI} . We use simple filter functions in l space to isolate different ranges of angular scales; a low pass, Gaussian filter

$$W_l^G(l_s) = \exp(-(l+1/2)^2/(l_s+1/2)^2) \quad (45)$$

⁵<http://www.netlib.org/slatec/src/>

⁶Based on an LCDM model with a scale-dependent (running) spectral index which best fits the dataset comprised of WMAP, CBI and ACBAR CMB data combined with 2dF and Ly- α data

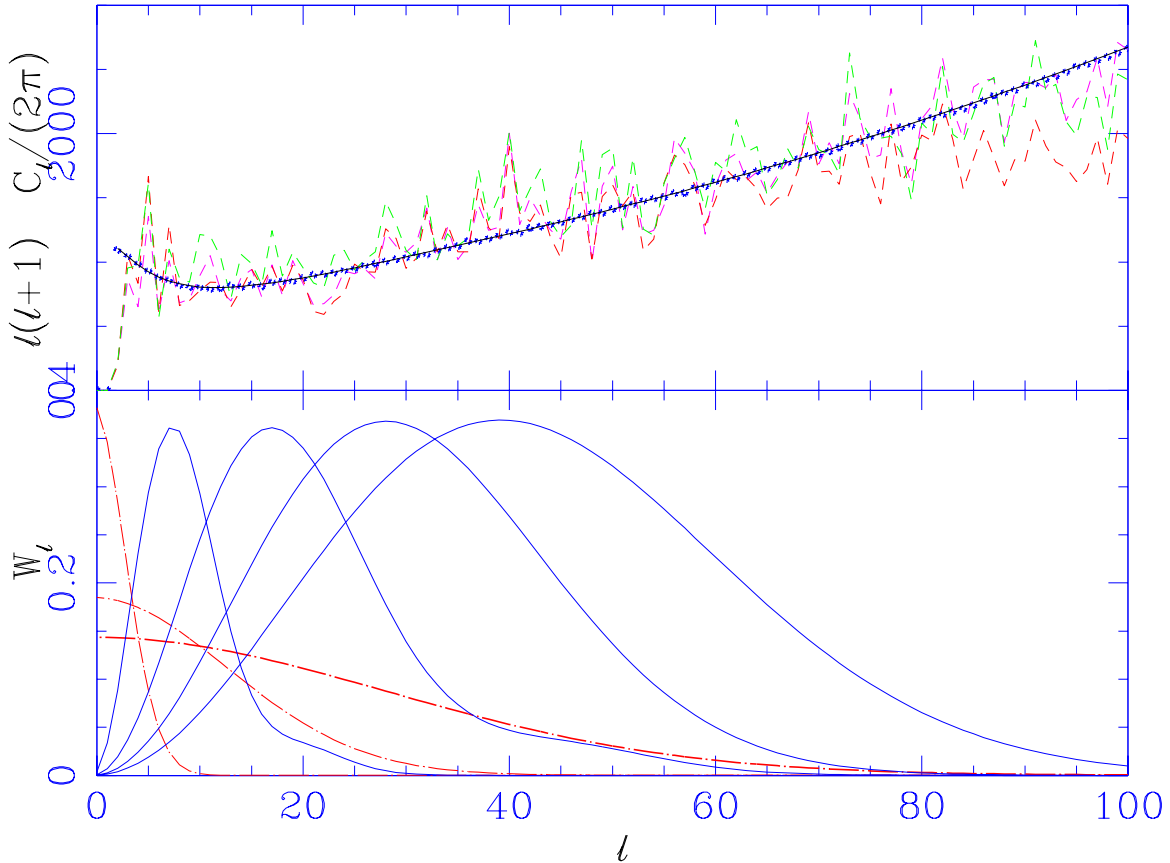


Figure 5: *Top*: C_ℓ of the two WMAP CMB anisotropy maps. The red, magenta and green curves correspond to map A, B and C, respectively. The black line is a ‘best fit’ WMAP theoretical C_ℓ used for simulating SI maps. Blue dots are the average C_ℓ recovered from 1000 realizations. *Bottom*: These plots show the window functions used. The dashed curves with increasing l coverage are ‘low-pass’ filter, $W_l^G(l_s)$, with $l_s = 4, 18, 40$, respectively. The solid lines are ‘band-pass’ filter $W_l^S(l_t, l_s)$ with $(l_s, l_t) = (13, 2), (30, 5), (30, 20), (45, 20)$, respectively.

that cuts off power on small angular scales ($\lesssim 1/l_s$) and a band pass filter,

$$W_l^S(l_t, l_s) = [2(1 - J_0((l + 1/2)/(l_t + 1/2)))] \exp(-(l + 1/2)^2/(l_s + 1/2)^2) \quad (46)$$

that retains power within a range of multipoles set by l_t and l_s . The windows are normalized such that $\sum_l (l + 1/2)/(l(l + 1)) W_l = 1$, i.e., unit *rms* for unit flat band power $C_l = 1/(l(l + 1))$. The window functions used in our work are plotted in figure 5. We use the C_l^T to generate 1000 simulations of the SI CMB maps. a_{lm} ’s are generated up to an l_{max} of 1024 (corresponding to HEALPix resolution $N_{side} = 512$). These are then multiplied by the window functions $W_l^G(l_s)$ and $W_l^S(l_t, l_s)$. We compute the BiPS for each realization. Fig.5 shows that the average power spectrum obtained from the simulation matches the theoretical power spectrum, C_l^T , used to generate the realizations. We use C_l^T to analytically compute bias and cosmic variance estimation for $\tilde{\kappa}_\ell$. This allows us to rapidly compute BiPS with 1σ error bars for different theoretical C_l^T .

We use the estimator given in eq.(36) to measure BiPS for the given CMB maps. We compute the BiPS for all window functions shown in Fig 5. Results for one these windows are plotted in Figs. 6. In the low- l regime, where we have kept the low multipoles, BiPS for all three given maps are consistent with zero. But in the intermediate- l regime (Fig. 6), although BiPS of ILC and TOH maps are well consistent with zero, the CSSK map shows a rising tail in BiPS due to the galactic mask. To confirm

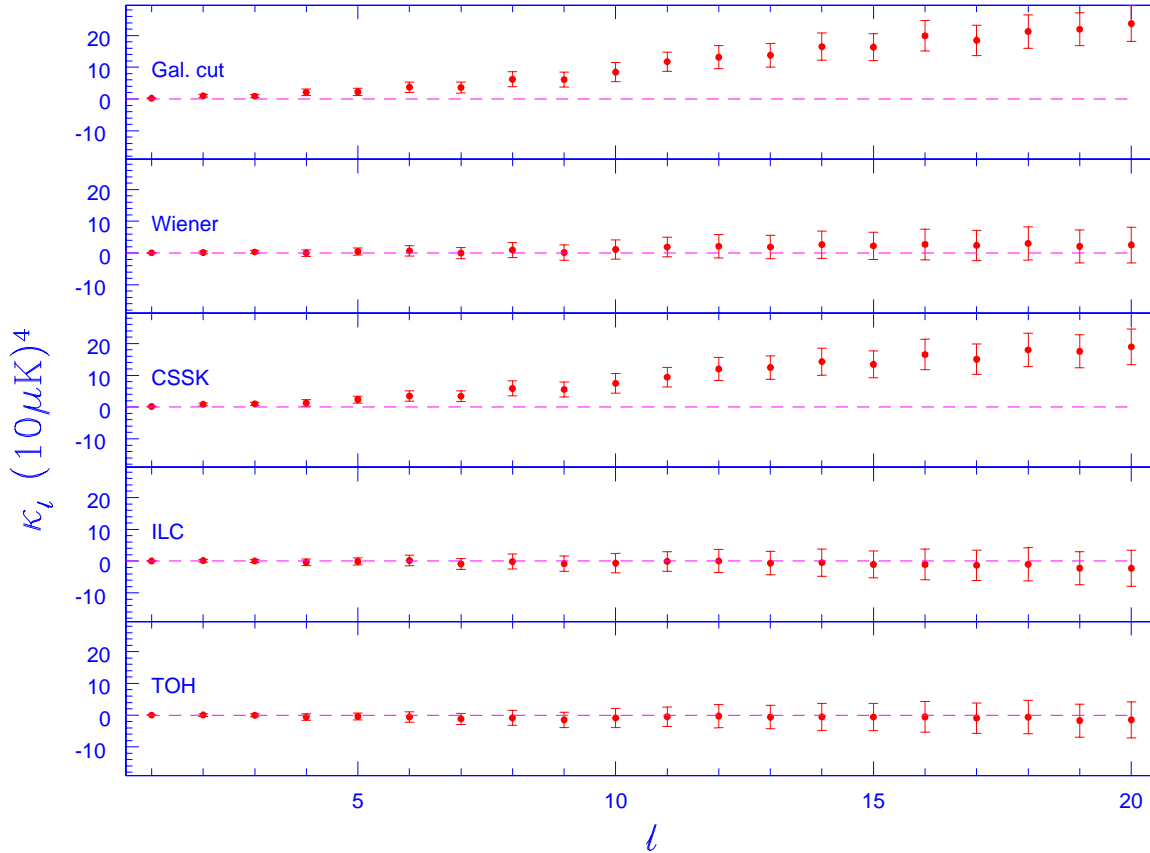


Figure 6: Measured BiPS for maps A, B and C filtered with a window with $l_s = 30$, $l_t = 20$. This is to check the statistical isotropy of the WMAP in the modest $20 < l < 40$ range in the multipole space where certain anomalies have been reported. ILC with a 10-degree-cut (top) has the same BiPS as map C ($l_s = 30$, $l_t = 20$) which explains that the raising tail of CSSK map is because of the mask.

it, we compute the BiPS for the ILC map with a 10-degree cut around the galactic plane (filtered with the same window function). The result is shown on the top panel of Fig. 6. Another interesting effect is seen when we apply a $W_l^S(20, 45)$ filter, where Wiener filtered map has a non zero BiPS very similar to that of CSSK but weaker. The reason is that Wiener filter takes out more modes from regions with more foregrounds since these are inconsistent with the theoretical model. As a result, a Wiener filtered map at $W_l^S(20, 45)$ filter has a BiPS similar to a cut sky map. The fact that Wiener map has less power at the Galactic plane can even be seen by eye! Hence using different filters allows us to uncover different types of violation of SI in a CMB map. In our analysis we have used a set of filters which enables us to probe SI breakdown on angular scales $l \lesssim 60$.

The BiPS measured from 1000 simulated SI realizations of C_l^T is used to estimate the probability distribution functions (PDF), $p(\tilde{\kappa}_\ell)$. A sample of the PDF for two windows is shown in Fig. 7. Measured values of BiPS for ILC, TOH and CSSK maps are plotted on the same plot. BiPS for ILC and TOH maps are located very close to the peak of the PDF. We compute the individual probabilities of the map being SI for each of the measured $\tilde{\kappa}_\ell$. This probability is obtained by integrating the PDF beyond the measured $\tilde{\kappa}_\ell$. To be precise, we compute

$$P(\tilde{\kappa}_\ell | C_l^T) = P(\kappa_\ell > \tilde{\kappa}_\ell) = \int_{\tilde{\kappa}_\ell}^{\infty} d\kappa_\ell p(\kappa_\ell), \quad \tilde{\kappa}_\ell > 0, \quad (47)$$

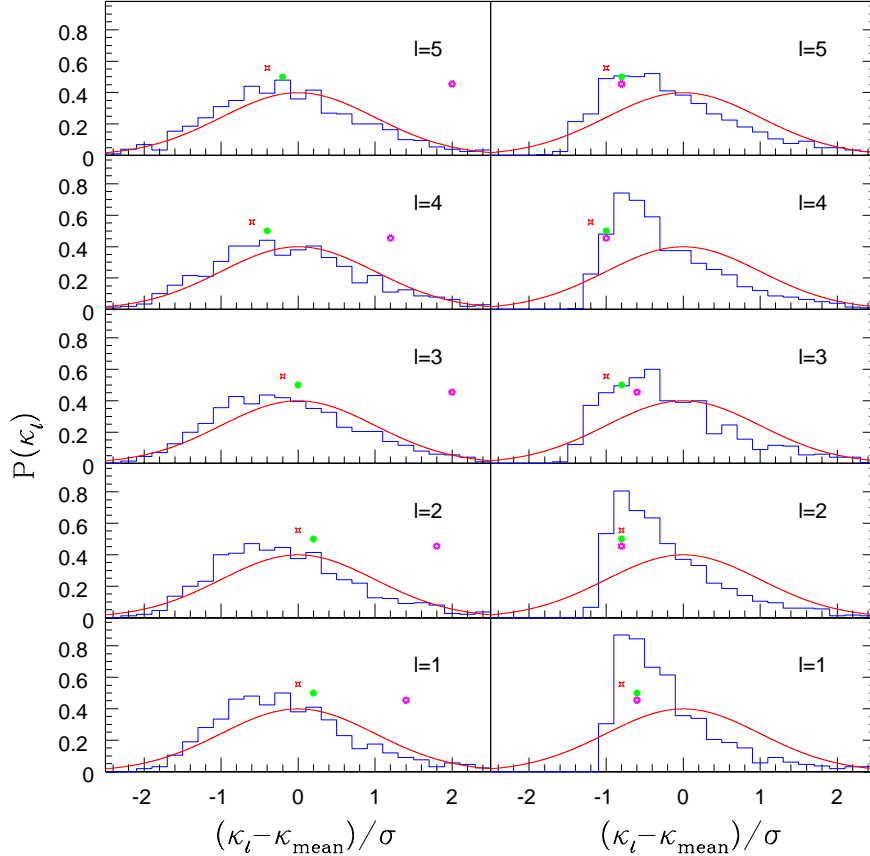


Figure 7: Probability distribution function for κ_1 to κ_5 constructed from 1000 realizations. The left panel shows the PDF for the maps filtered with $W_l^S(20, 30)$ (left panel) and $W_l^G(l_s = 40)$ (right panel). The latter is more skewed, which explains the apparent $\sim 1\sigma$ shift in the κ_ℓ values for $W_l^G(l_s = 40)$ at low ℓ . The green, magenta and red (circular, pentagonal and rectangular) points represent ILC, CSSK and TOH maps, respectively. The smooth solid curves are Gaussian approximations.

$$= P(\kappa_\ell < \tilde{\kappa}_\ell) = \int_{-\infty}^{\tilde{\kappa}_\ell} d\kappa_\ell p(\kappa_\ell), \quad \tilde{\kappa}_\ell < 0.$$

The probabilities obtained are shown in Figs. 4 and 4 for $W_l^S(20, 30)$, $W_l^G(40)$ and $W_l^G(4)$. The probabilities for the $W_l^S(20, 30)$ window function are greater than 0.25 and the minimum probability at ~ 0.05 occurs at κ_4 for $W_l^G(40)$. The reason for systematically lower SI probabilities for $W_l^S(20, 30)$ as compared to $W_l^G(40)$ is simply due to lower cosmic variance of the former. The contribution to the cosmic variance of BiPS is dominated by the low spherical harmonic multipoles. Filters that suppress the a_{lm} at low multipoles have a lower cosmic variance.

It is important to note that the above probability is a conditional probability of measured $\tilde{\kappa}_\ell$ being SI given the theoretical spectrum C_l^T (used to estimate the bias). A final probability emerges as the Bayesian chain product with the probability of the theoretical C_l^T used given data. Hence, small difference in these conditional probabilities for the two maps are perhaps not necessarily significant. Since the BiPS is close to zero, the computation of a probability marginalized over the C_l^T may be possible using Gaussian (or, improved) approximation to the PDF of κ_ℓ .

The important role played by the choice of the theoretical model for the BiPS measurement is shown for a W_l that retains power in the lowest multipoles, $l = 2$ and $l = 3$. Assuming C_l^T , there are hints of non-

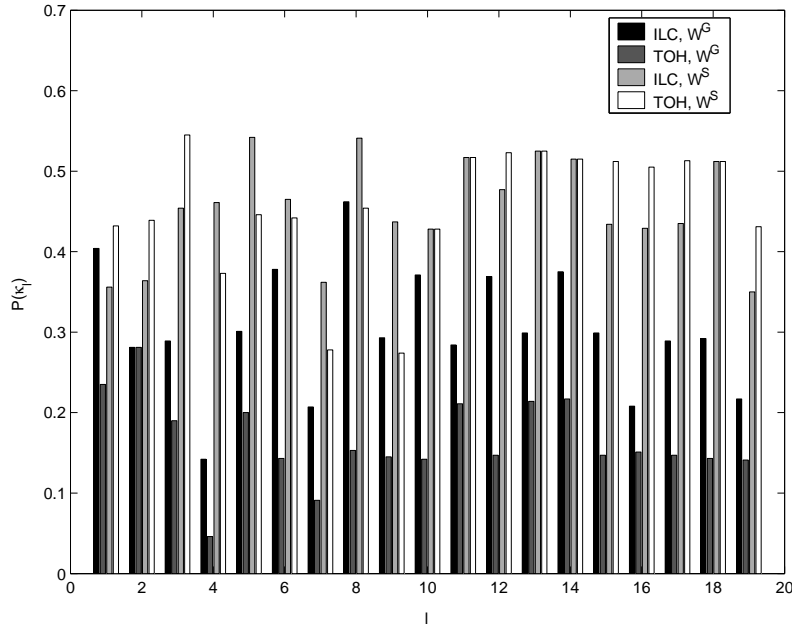


Figure 8: The probability of two of the *WMAP* based CMB maps being SI when filtered by $W_l^S(20, 30)$ and a Gaussian filter $W_l^G(40)$.

SI detections in the low ℓ 's (top-left panel of Fig. 9). We also compute the BiPS using a C_l^T for a model that accounts for suppressed quadrupole and octopole in the *WMAP* data [Shafieloo & Souradeep 2004]. The mild detections of a non zero BiPS vanish for this case (top-right panel of Fig. 9). The corresponding SI probabilities for the two choices of C_l^T are shown in the lower panels.

5 Discussion and Conclusion

The SI of the CMB anisotropy has been under scrutiny after the release of the first year of *WMAP* data. We use the BiPS which is sensitive to structures and patterns in the underlying total two-point correlation function as a statistical tool of searching for departures from SI. We carry out a BiPS analysis of *WMAP* full sky maps. We find no strong evidence for SI violation in the *WMAP* CMB anisotropy maps considered here. We have verified that our null results are consistent with measurements on simulated SI maps. The BiPS measurement reported here is a Bayesian estimate of the conditional probability of SI (for each κ_ℓ of the BiPS) given an underlying theoretical spectrum C_l^T . We point out that the excess power in the C_l^T with respect to the measured C_l from *WMAP* at the lowest multipoles tends to indicate mild deviations from SI. BiPS measurements are shown to be consistent with SI assuming an alternate model C_l^T that is consistent with suppressed power on low multipoles. Note that it is possible to band together κ_ℓ measurements to tighten the error bars further. The full sky maps and the restriction to low $l < 60$ (where instrumental noise is sub-dominant) permits the use of our analytical bias subtraction and error estimates. The excellent match with the results from numerical simulations is a strong verification of the numerical technique. This is an important check before using Monte-Carlo simulations in future work for computing BiPS from CMB anisotropy sky maps with a galactic mask and non uniform noise matrix.

There are strong theoretical motivations for hunting for SI violation in the CMB anisotropy. The possibility of non-trivial cosmic topology is a theoretically well motivated possibility that has also been observationally targeted [Ellis 1971, Lachieze-Rey & Luminet 1995, Levin 2002, Linde 2004]. The breakdown of statistical homogeneity and isotropy of cosmic perturbations is a generic feature of ultra large scale structure of the cosmos, in particular, of non trivial cosmic topology [Bond, Pogosyan & Souradeep 1998, 2000].

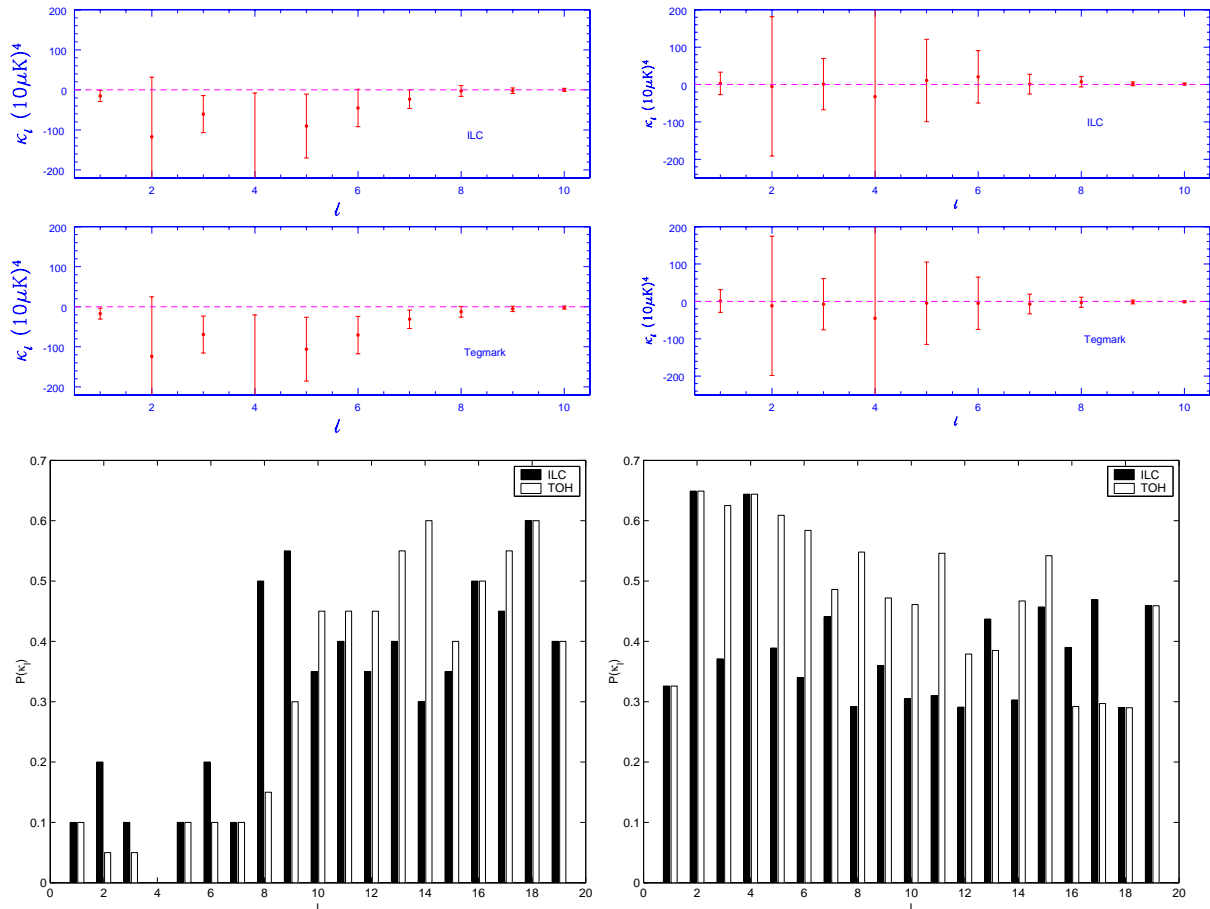


Figure 9: **Top;** Figure compares the measured values of κ_ℓ for maps A and B filtered to retain power only on the lowest multipoles, $l = 2$ and $l = 3$ assuming the WMAP theoretical spectrum WMAPbf (*left*) and a model spectrum that matches the suppressed power at the lowest multipoles [Shafieloo & Souradeep 2004]. The non zero κ_ℓ ‘detections’ assuming the WMAP theoretical spectrum become consistent with zero for a C_l^T that has power suppressed at low multipoles. **Bottom:** The corresponding SI probability assuming the WMAP theoretical spectrum, C_l^T (*left*) and a model spectrum that matches the suppressed power at the lowest multipoles (*right*).

The underlying correlation patterns in the CMB anisotropy in a multiply connected universe is related to the symmetry of the Dirichlet domain. The BiPS expected in flat, toroidal models of the universe has been computed and shown to be related to the principle directions in the Dirichlet domain [Hajian & Souradeep 2003a]. As a tool for constraining cosmic topology, the BiPS has the advantage of being independent of the overall orientation of the Dirichlet domain with respect to the sky. Hence, the null result of BiPS can have important implication for cosmic topology. This approach complements direct search for signature of cosmic topology [Cornish, Spergel & Starkman 1998, de Oliveira-Costa et al. 1996] and our results are consistent with the absence of the matched circles and the null S-map test of the WMAP CMB maps [Cornish et al. 2003, de Oliveira-Costa et al. 2003]. Full Bayesian likelihood comparison to the data of specific cosmic topology models is another approach that has applied to COBE-DMR data [Bond, Pogossyan & Souradeep 1998, 2000]. Work is in progress to carry out similar analysis on the large angle WMAP data. We defer to future publication, detailed analyzes and constraints on cosmic topology using null BiPS measurements, and the comparison to the results from complementary approaches. There are also other theoretical scenarios that predict breakdown of SI that can be probed using BiPS, e.g., primordial cosmological magnetic fields [Durrer et al. 1998, Chen et al. 2004].

The null BiPS results also has implications for the observation and data analysis techniques used to create the CMB anisotropy maps. Observational artifacts such as non-circular beam, inhomogeneous noise correlation, residual stripping patterns, etc. are potential sources of SI breakdown. Our null BiPS results confirm that these artifacts do not significantly contribute to the maps studied here. Foreground residuals can also be sources of SI breakdown. The extent to which BiPS probes foreground residuals is yet to be fully studied and explored. We do not see any significant effect of the residual foregrounds in ILC and the TOH maps as it was mentioned by [Eriksen et al. 2004c]. This can not be necessarily called a discrepancy between the two results unless we know what should have been seen in the BiPS. The question is if the signal is strong enough and whether the effect smeared out in bipolar multipole space within our angular l -space window. On the other hand, the very fact that BiPS does show a strong signal for the Wiener filtered map, mean that at some level BiPS is sensitive to galactic residuals.

In summary, we study the Bipolar power spectrum (BiPS) of CMB which is a promising measure of SI. We find null measurements of the BiPS for a selection of full sky CMB anisotropy maps based on the first year of WMAP data. Our results rule out radical violation of statistical isotropy in the CMB anisotropy measured by WMAP.

References

- [Bamba et al. 2004] Bamba, K., Yokoyama, J., Phys.Rev. D69 (2004) 043507.
- [Bardeen et al. 1983] Bardeen, J. M., Steinhardt, P. J. & Turner, M. S. 1983, Phys. Rev. D 28, 679.
- [Bartolo et al. 2004] Bartolo, N., Komatsu, E., Matarrese, S., Riotto, A., *preprint* (astro-ph/0406398)
- [Bennett et al. 2003] Bennett, C. L., et.al., 2003, Astrophys. J. Suppl., **148**, 1.
- [Bond 2004] Bond, J. R. et al. 2004, Int. J. Theor. Phys. 2004, ed. Verdaguer, E., "The Early Universe: Confronting theory with observations" (June 21-27, 2003) (astro-ph/0406195).
- [Bond,Pogosyan & Souradeep 1998,2000] Bond, J. R., Pogosyan, D. & Souradeep,T. 1998, Class. Quant. Grav. **15**, 2671; *ibid.* 2000, Phys. Rev. **D 62**,043005;2000, Phys. Rev. **D 62**,043006.
- [Chen et al. 2004] Chen, G., Mukherjee, P., Kahniashvili, T., Ratra, B., Wang, Y., Astrophys.J. 611 (2004) 655.
- [Coles 2003] Coles, P. et al. 2003, *preprint* (astro-ph/0310252).
- [Copi et al. 2004] Copi, C. J., Huterer, D. & Starkman, G. D. 2004, Phys. Rev. D. *in press*, (astro-ph/0310511).
- [Cornish,Spergel & Starkman 1998] Cornish, N.J., Spergel, D.N. & Starkman, G. D. 1998, Class. Quantum Grav., **15**, 2657
- [Cornish et al. 2003] Cornish, N. J., Spergel, D., Starkman, G. , Komatsu, E., 2004, Phys.Rev.Lett. 92, 201302.
- [Cruz et al. 2004] Cruz, M., Martinez-Gonzalez, E., Vielva, P., Cayon, L., *preprint* (astro-ph/0405341).
- [de Oliveira-Costa et al. 2003] de Oliveira-Costa, A., Tegmark, M., Zaldarriaga, M. & Hamilton, A. 2004, Phys. Rev.**D69**, 063516.
- [de Oliveira-Costa et al. 1996] de Oliveira-Costa, A. Smoot, G. F., Starobinsky, A. A., 1996, ApJ **468**, 457.
- [Dineen et al. 2004] Dineen, P. , Rocha, G., Coles, P, *preprint* (astro-ph/0404356).
- [Donoghue et al. 2004] Donoghue, E. P., and Donoghue, J. F., *preprint* (astro-ph/0411237).
- [Durrer et al. 1998] Durrer, R., Kahniashvili, T. and Yates, A., 1998, Phys. Rev. **D 58**, 3004.

- [Ellis 1971] Ellis, G. F. R. 1971, *Gen. Rel. Grav.* **2**, 7.
- [Eriksen et al. 2004a] Eriksen, H. K. et al., 2004, *Astrophys. J* **605**, 14.
- [Eriksen et al. 2004b] Eriksen, H. K. et al., 2004, *Astrophys. J.* **612**, 64.
- [Eriksen et al. 2004c] Eriksen, H. K. et al., 2004, *Astrophys. J.* **612**, 633.
- [Gaztanaga & Wagg 2003] Gaztanaga, E. & Wagg, J. 2003, *Phys. Rev.* **D68** 021302.
- [Górski,Hivon & Wandelt 1999] Górski,K. M., Hivon, E., Wandelt, B. D. 1999, in "Evolution of Large-Scale Structure", eds. A.J. Banday, R.S. Sheth and L. Da Costa, PrintPartners Ipskamp, NL, pp. 37-42 (also astro-ph/9812350).
- [1] J. R. Gott 1980. *Mon. Not. R. Astr. Soc.* **193**, 153.
- [Guth & Pi 1982] Guth, A. H. & Pi, S.-Y. 1982, *Phys. Rev. Lett.*, 49, 1110.
- [Hajian & Souradeep 2003a] Hajian, A. & Souradeep, T., 2003 *preprint* (astro-ph/0301590).
- [Hajian & Souradeep 2003b] Hajian, A. and Souradeep, T., 2003b, *ApJ* 597, L5 (2003).
- [Hajian & Souradeep 2005a] Hajian, A. & Souradeep, T., 2005, *ApJ* 618, L63.
- [Hajian & Souradeep 2005b] Hajian, A. & Souradeep, 2005, *preprint* (astro-ph/0501001)
- [Hajian et al. 2004] Hajian, A., Pogosyan, D. Souradeep, T., Contaldi, C., Bond, R., 2004 *in preparation*; Proc. 20th IAP Colloquium on Cosmic Microwave Background physics and observation, 2004.
- [Hajian et al. 2004b] Hajian, A., Chen, G., Souradeep, T., Kahnianashvilli, T., Ratra, B., 2004 *in preparation*.
- [Hansen et al. 2004] Hansen, F. K., Banday, A. J. & Gorski, K. M. 2004, *preprint*. (astro-ph/0404206)
- [Hinshaw et al. 2003] G. Hinshaw, *Astrophys. J. Suppl.*,(2003) ,**148**, 135.
- [Komatsu et al. 2003] Komatsu, E. et.al., 2003, *ApJS*, **148**, 119.
- [Kogut et al. 2003] Kogut A. et al., 2003, *Astrophys. J. Suppl.*,**148**, 161.
- [Lachieze-Rey & Luminet 1995] Lachieze-Rey, M. and Luminet,J. -P. 1995, *Phys. Rep.* **25**, 136.
- [Larson & Wandelt 2004] Larson, D. L. & Wandelt, B. D. 2004, *preprint*, (astro-ph/0404037).
- [Levin 2002] Levin, J. 2002, *Phys. Rep.* **365**, 251.
- [Levin et al. 1998] Levin J., Scannapieco E., Silk J., (1998), *Class.Quant.Grav.* 15, 2689.
- [Linde 2004] Linde, A., (2004), *JCAP* 0410, 004, (astro-ph/0408164).
- [Luminet et al. 2003] Luminet, J.-P. et al. 2003, *Nature* 425 593.
- [Ma & Bertschinger 1995] Ma, C.-P., & Bertschinger, E. 1995, *ApJ*, 455, 7
- [Mitra et al. 2004] Mitra, S., Sengupta, A., S., Souradeep, T.,*preprint* astro-ph/0405406
- [Munshi et al. 1995] Munshi, D., Souradeep, T., and Starobinsky, A. A., (1995), *Astrophys. J.*, 454, 552.
- [Page et al. 2003] Page L. et al., 2003, *Astrophys. J. Suppl.*,**148**, 233.
- [Naselsky et al. 2004] Naselsky et al, 2004, *preprint*, (astro-ph/0405523); *ibid* (astro-ph/0405181), 2003; *ApJ*,599,L53 and references therein.
- [Park 2004] Park, C., 2004, *Mon. Not. Roy. Astron. Soc.* **349**, 313.

- [Peiris et al., 2003] Peiris H.V. et al., 2003, *Astrophys. J. Suppl.*, **148**, 213.
- [Prunet et al. 2004] Prunet, S., Uzan, J., Bernardeau, F., Brunier, T., 2004, *preprint* (astro-ph/0406364).
- [Ratra 1992] Ratra, B., (1992), *Astrophys.J.* 391, L1.
- [Sachs and Wolfe, 1967] Sachs, R. K., and Wolfe, A. M. 1967, *ApJ*, 147, 73.
- [Schwarz et al. 2004] Schwarz, D. J. et al., 2004, *preprint* (astro-ph/0403353).
- [Shafieloo & Souradeep 2004] Shafieloo, A. & Souradeep, T., 2004, *Phys. Rev. D*, *in press*, (astro-ph/0312174).
- [Sokolov & Shvartsman 1974] D. D. Sokolov and V. F. Shvartsman (1974) *Zh. Eksp. Theor. Fiz.* **66**, 412 [*JETP*, **39**, 196 (1974)].
- [Souradeep 2000] Souradeep, T. 2000, in ‘The Universe’, eds. Dadhich, N. & Kembhavi, A., Kluwer.
- [Souradeep & Hajian 2003] Souradeep, T. and Hajian, A., 2004, *Pramana*, **62**, 793.
- [Spergel et al. 2003] Spergel, D. et al., 2003, *Astrophys. J. Suppl.*, **148**, 175.
- [Spergel et al. 1999] Spergel, D., and Goldberg, D. M., (1999), *Phys.Rev.* D59, 103001.
- [Starkman 1998] Starkman, G. *Class. 1998, Quantum Grav.* **15**, 2529.
- [Starobinsky 1982] Starobinsky, A. A. 1982, *Phys. Lett*, 117B, 175.
- [Tegmark et al. 2004] Tegmark, M., de Oliveira-Costa, A. & Hamilton, A., 2004, *Phys.Rev.* **D68** 123523.
- [Varshalovich et al. 1988] Varshalovich, D. A., Moskalev, A. N., Khersonskii, V. K., 1988 *Quantum Theory of Angular Momentum* (World Scientific).
- [Vielva et al. 2003] Vielva, P., Martinez-Gonzalez, E., Barreiro, R. B., Sanz, J. L., Cayon, L., 2003, *preprint* (astro-ph/0310273).
- [Zaldarriaga et al. 1998] Zaldarriaga, M., Seljak, U., Bertschinger, E., 1998, *Astrophys. J.*, **494**, 491.